

AD-A275 793



62

ARMY RESEARCH LABORATORY



Characterization of a Diffraction Grating as a Simulant of a Selective Frequency Antenna for Radiometric Applications

by Thomas J. Pizzillo

ARL-TR-303

January 1994

DTIC
ELECTE
FEB 14 1994
S E D

DTIC QUALITY INSPECTED 8

2096 94-04925



9 4 2 10 24 9
Approved for public release; distribution unlimited

The findings in this report are not to be construed as an official Department of the Army position unless so designated by other authorized documents.

Citation of manufacturer's or trade names does not constitute an official endorsement or approval of the use thereof.

Destroy this report when it is no longer needed. Do not return it to the originator.

REPORT DOCUMENTATION PAGE			<i>Form Approved</i> <i>OMB No. 0704-0188</i>	
<small>Public reporting burden for this collection of information is estimated to average 1 hour per response, including the time for reviewing instructions, searching existing data sources, gathering and maintaining the data needed, and completing and reviewing the collection of information. Send comments regarding this burden estimate or any other aspect of this collection of information, including suggestions for reducing this burden, to Washington Headquarters Services, Directorate for Information Operations and Reports, 1215 Jefferson Davis Highway, Suite 1204, Arlington, VA 22202-4302, and to the Office of Management and Budget, Paperwork Reduction Project (0704-0188), Washington, DC 20503.</small>				
1. AGENCY USE ONLY (Leave blank)		2. REPORT DATE January 1994	3. REPORT TYPE AND DATES COVERED Final, from Oct 1991 to Oct 1992	
4. TITLE AND SUBTITLE Characterization of a Diffraction Grating as a Simulant of a Selective Frequency Antenna for Radiometric Applications			5. FUNDING NUMBERS DA PR: 61102.AH43 PE: 611102.H43	
6. AUTHOR(S) Thomas J. Pizzillo				
7. PERFORMING ORGANIZATION NAME(S) AND ADDRESS(ES) U.S. Army Research Laboratory Attn: AMSRL-SS-SH 2800 Powder Mill Road Adelphi, MD 20783-1197			8. PERFORMING ORGANIZATION REPORT NUMBER ARL-TR-303	
9. SPONSORING/MONITORING AGENCY NAME(S) AND ADDRESS(ES) U.S. Army Research Laboratory 2800 Powder Mill Road Adelphi, MD 20783-1197			10. SPONSORING/MONITORING AGENCY REPORT NUMBER	
11. SUPPLEMENTARY NOTES ARL PR: 611102				
12a. DISTRIBUTION/AVAILABILITY STATEMENT Approved for public release; distribution unlimited.			12b. DISTRIBUTION CODE	
13. ABSTRACT (Maximum 200 words) This report details the study of a blazed diffraction grating as a simulant of a selective frequency antenna for radiometric applications. Specifically, the ability to direct and sweep a beam of millimeter-wave (MMW) energy is explored as a potential means of munitions guidance. A grating was designed and built to direct incident energy into the negative first-order peak of the associated diffraction spectrum. A change of 1 GHz in the incident energy frequency is shown to produce a beam displacement of 0.3°, a polarization dependence is shown to exist for energy in orders other than zero, and a limited scaling of the optical theory of diffraction to MMW energies is demonstrated to be feasible.				
14. SUBJECT TERMS Millimeter wave, diffraction grating, antenna, radiometer			15. NUMBER OF PAGES 20	
			16. PRICE CODE	
17. SECURITY CLASSIFICATION OF REPORT Unclassified	18. SECURITY CLASSIFICATION OF THIS PAGE Unclassified	19. SECURITY CLASSIFICATION OF ABSTRACT Unclassified	20. LIMITATION OF ABSTRACT UL	

Contents

1. Introduction	5
2. Background	6
3. Instrumentation	9
4. Experimental Procedure	12
5. Results	13
6. Conclusions	18
Acknowledgments	18
Distribution	19

Figures

1. Spectrum due to a diffraction grating	7
2. Schematic representation of interference and diffraction dependence on grate parameters	8
3. Spectrum due to a blazed grating	8
4. Instrumentation diagram	9
5. Geometry of grate used for reported data	10
6. Measurement geometry	12
7. Calibration measurement of flat aluminum plate	13
8. 0 to 90° measurement of grate	14
9. $m = -1$ of figure 8	15
10. $m = 0$ of figure 8	15
11. $m = 1$ of figure 8	15
12. 15° polarization measurement	16
13. 30° polarization measurement	16
14. 45° polarization measurement	17

Tables

1. Calibration plot parameters	13
2. Figure 8 peak parameters	16
3. Peak power polarization dependence for angles 15°, 30°, and 45°	17

1. Introduction

The U.S. Army is investigating millimeter-wave (MMW) radiation as a means of guiding munitions. A crucial aspect of a guidance system is its ability to detect and track a target. This requires a radar, for transmitting/receiving the energy, and an antenna, mounted on high-precision gimbals, for steering the radiation in space. Alternatively, detection can be done by a radiometer, which discriminates the cold space temperature reflected off a target from the much hotter terrestrial background. The use of a frequency-selective antenna allows for passive scanning. This system would discern where in its field of view (FOV) a target is by narrowpass filtering the received broadband signal. Many narrowpass filters could be used to generate a line scan image of the FOV for target identification. A simpler system, consisting of only two filters, could be used in applications where complete images are not required, such as final in-flight trajectory corrections for tube-launched munitions. If an MMW beam is used to steer them in this manner, future smart munitions could be smaller and less susceptible to environmental factors such as launch dynamics. This report details the investigation of a diffraction grating as a simulant for a frequency-selective antenna.

Accession For	
NTIS CRA&I	<input checked="" type="checkbox"/>
DTIC TAB	<input type="checkbox"/>
Unannounced	<input type="checkbox"/>
Justification	
By	
Distribution /	
Availability Codes	
Dist	Avail and/or Special
A-1	

DTIC QUALITY INSPECTED 2

2. Background

The principle behind diffraction gratings is well documented and described in any of a number of optics books.¹ The specific phenomenon exploited is diffraction of electromagnetic radiation by a grating of reflecting facets. The spectrum produced by a diffraction grating is created by two distinct phenomena: interference and diffraction. It can be calculated from the general grating equation,

$$l(\sin \theta_m - \sin \theta_i) = m\lambda , \quad (1)$$

where

- θ_m = angle of m^{th} order peak relative to the surface normal,
- θ_i = incident angle of transmitted radiation,
- l = facet separation,
- m = m^{th} order interference peak, and
- λ = wavelength of incident radiation.

Figure 1 demonstrates how the combination of an interference pattern (top of figure) with a diffraction pattern (middle) produces the observed spectrum of a diffraction grating (bottom). The angular distribution of the orders is determined by the interference of radiation from multiple facets. It is dependent on both frequency and facet spacing. Hence, equation (1) may be used to determine the location of the interference orders for a given angle of incidence. The interference is due to specular reflection from the surface as a whole and is constrained by

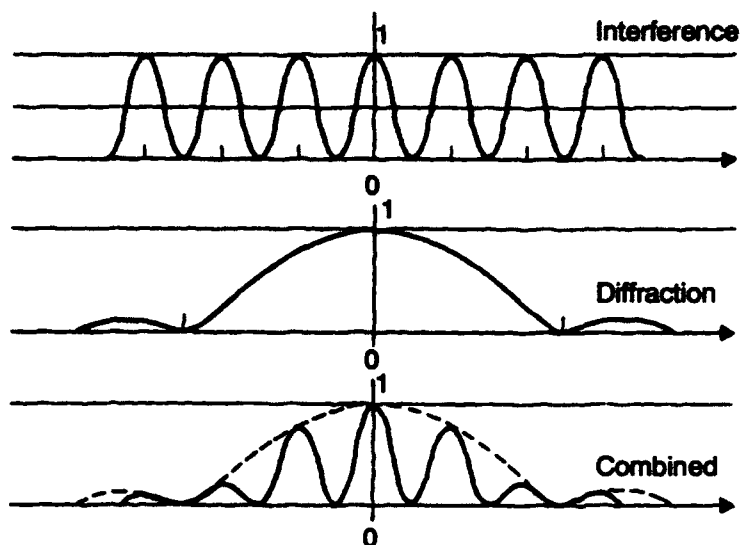
$$\theta_i = \theta_o , \quad (2)$$

where θ_o is the angle of reflection. Diffraction from a single facet is also a specular reflection and determines the location of the diffraction peak.

The combined spectrum is of little use with a standard grating because of the spreading, by diffraction, of the energy into multiple interference orders or beams. For purposes of steering radiation, a particular type of reflection grating, a blazed grating, is required. Blazing refers to the angling of the reflecting facets of the grate relative to the surface normal. This angle is referred to as the blaze angle, θ_b . Blazing eliminates the unwanted spreading over multiple orders by directing most of the incident energy into only one of the interference maxima. The blazed spectrum can be accounted for by two effects: interference of radiation from multiple facets and dif-

¹For example, Miles V. Klein and Thomas E. Furtak, *Optics*, Wiley, New York (1986).

Figure 1. Spectrum due to a diffraction grating. Interference function multiplied with diffraction function produces observed, combined function. (Figure adapted from Klein and Furtak.)



fraction of radiation from a single facet. Figure 2 gives a schematic representation of these two effects. The location of the diffraction peak is measured relative to the normal of a single facet and is indicated as θ_0 (the minus indicates that the angles are on the same side of the surface normal):

$$\theta_i - \theta_0 = 2\theta_b . \quad (3)$$

Hence, varying the frequency of radiation incident on a blazed diffraction grating allows a single MMW beam to be directed and swept in a particular region of space. Figure 3 shows the blazed spectrum as a function of the dimensionless parameter λ_b/l where λ_b is the "tuned" wavelength of the grate. The tuned wavelength is defined as the wavelength corresponding to $m = 1$ in equation (1). Varying λ , the incident wavelength, moves the diffraction pattern relative to the interference pattern, enhancing one or another of the interference maxima. To determine the feasibility of using frequency-selective surfaces as a method for steering radiation, ARL designed an experiment to measure this effect.

Figure 2. Schematic representation of interference and diffraction dependence on grate parameters.

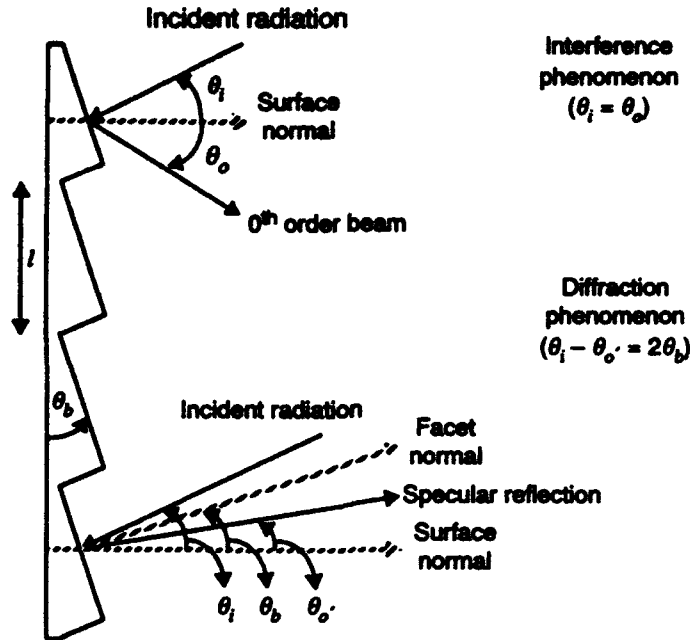
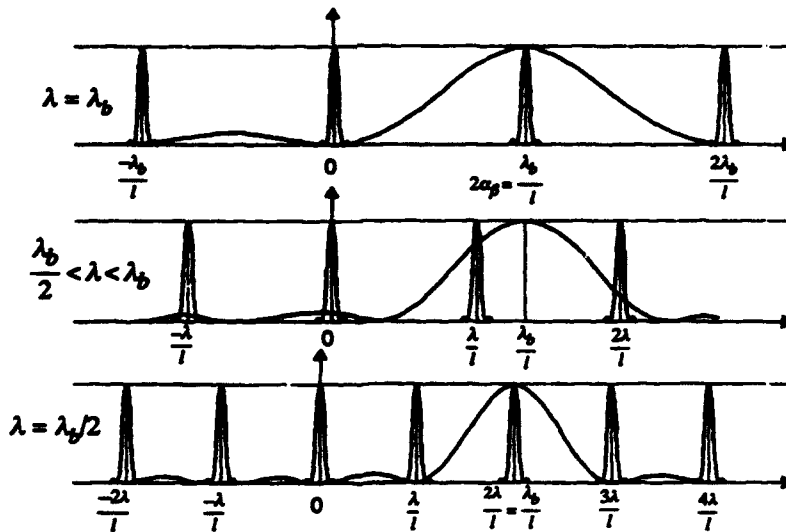


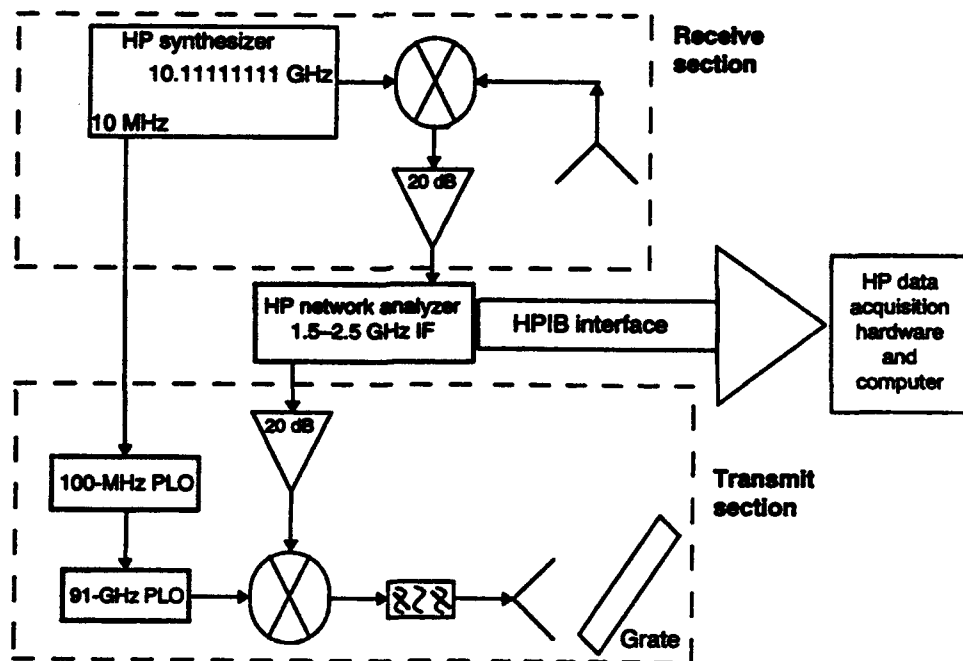
Figure 3. Spectrum due to a blazed grating: (top) spectrum for $m = 1$, i.e., incident radiation equals "tuned" frequency of grate; (bottom) spectrum for $m = 2$, i.e., incident radiation is twice tuned frequency; (center) radiation between these two. For integer values of m , zeroes in diffraction pattern cancel all other peaks in interference pattern. (Figure adapted from Klein and Furtak.)



3. Instrumentation

The radar instrumentation, the data acquisition software, and the radar control software were developed and fabricated by ARL. The instrumentation, diagrammed in figure 4, consisted of a bistatic frequency-modulated (FM), continuous wave (cw) 93-GHz transmissometer, a diffraction grating, and Hewlett-Packard (HP) data acquisition and signal synthesis equipment. The transmitter consisted of a 91-GHz phase-locked oscillator (PLO) locked to a 100-MHz PLO. A variable IF signal, 1.5 to 2.5 GHz, at -10 dBm was generated by the HP network analyzer, amplified, and then mixed in a single-sideband up-converter with the output from the 91-GHz PLO. The mixed signal passed through a filter and then was transmitted towards the grating via a 5-cm circular antenna at a power of 0 dBm. The receiver intercepted the radiation reflected from the grate using a 15-cm circular antenna feeding a harmonic mixer. The mixer down-converted the received signal using the ninth harmonic of the source generated by an HP frequency synthesizer. The synthesizer and source were kept coherent by the oscillator being locked to a 10-MHz reference signal from the synthesizer. A low-noise preamplifier was used on the harmonic mixer to set the system noise figure before processing by the HP network analyzer. The difference signal

Figure 4. Instrumentation diagram.



generated by the network analyzer could not be coherently integrated directly. Because of the limited resolution of the synthesizer, the phase of the down-converted signal continuously drifted in time. Therefore, a fast Fourier transform (FFT) was performed on the difference signal, and the maximum amplitude was recorded. This peak corresponds to the beat frequency between the transmitted signal and the resolution-limited harmonic, specifically, 8 Hz. An HP computer system was used to control the radar and perform data acquisition.

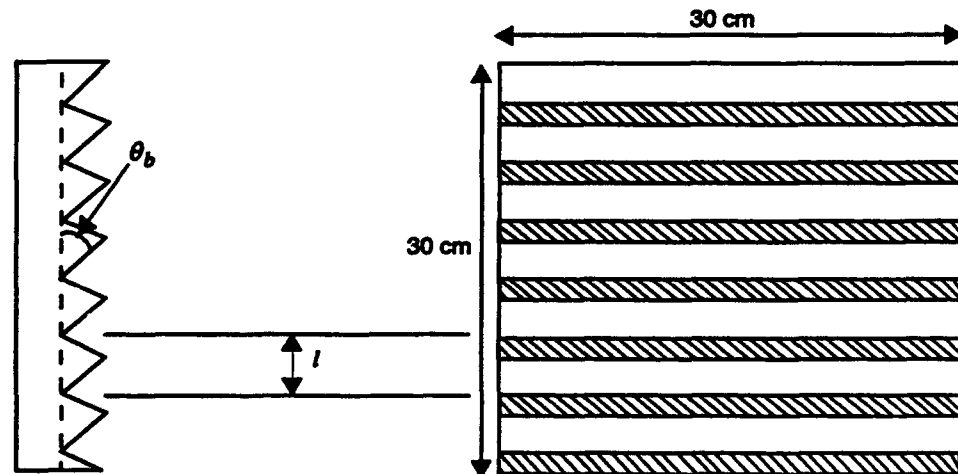
A number of gratings were studied, each with its own specific geometry. The data presented in this report were obtained with the grate geometry in figure 5. The overall dimensions are 30 by 30 cm. The blaze angle, θ_b , is 14.5° . Facet spacing, l , is 4.84 mm, allowing for 61 facets to be machined across the face of the aluminum.

The following guidelines are proffered for creating MMW blazed diffraction gratings. Given a fixed θ_i and taking the derivative of equation (1) with respect to λ and θ_m , we define the angular dispersion,

$$\frac{d\theta_m}{d\lambda} = \frac{m}{l \cos \theta_m} \quad (4)$$

where $d\theta_m$ corresponds to the amount of shift required and $d\lambda$ is the corresponding change in wavelength. The cosine argument is now the location of the receiver relative to the grate normal as a function of the integer value m and facet separation l . The facet separation should be greater than a single wavelength: two or three times greater is preferable. The order is then chosen so that the angular dispersion requirement is met; the higher the value of m , the further

Figure 5. Geometry of grate used for reported data.



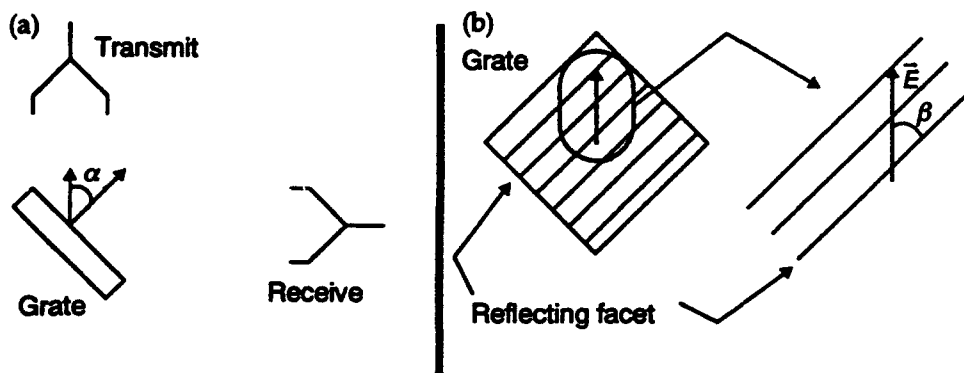
apart different frequency peaks will be. However, the measurement becomes more difficult, because the angle between transmitter and receiver is also increased until shadowing effects are significant. Shadowing effects occur when the top of one facet blocks a significant portion of a neighboring facet, and edge diffraction begins to dominate the spectrum. Once a value of m is determined, and hence θ_m , equation (3) may be used to determine θ_b , blaze angle, which is used in the manufacture of the grate. It is recommended when the grate is made that mill tolerances be kept tight to avoid surface anomalies. I found that noise increased significantly when a less than precise mill was used in making some of the initial gratings.

4. Experimental Procedure

Figure 6 shows the measurement geometry. The grate was mounted so that rotations could be made in two dimensions: rotation in the plane defined by the grate normal and the bore of the transmit antenna, as shown in figure 6a, and rotation in a plane defined by the reflecting facets and the incident electric field polarization, as shown in figure 6b. Figure 6a is the plane for measurements of field strength as a function of radiation angle of incidence, and figure 6b is the plane for polarization measurements. The transmit antenna was set 61 cm from the grate illuminating the center region. The receive antenna was positioned 15.25 m from the grate with its bore perpendicular to the transmitter's bore. All three components were oriented in a common plane.

Measurements were made with the polarization angle (defined in fig. 6b) fixed, and the angle of incidence (defined in fig. 6a) varied. Readings could be acquired in steps of 0.1° with the normal of the grate surface passing from 0 to 90° as defined by α . At each angle increment, the frequency was stepped from 1.5 to 2.5 GHz in steps of 100 MHz.

Figure 6.
Measurement geometry: (a) α indicates angle of incident radiation, and (b) β indicates angle of incident polarization.



5. Results

To determine the angle between transmitter and receiver, I first covered the diffraction surface with a flat aluminum plate. The plate was rotated from 0 to 90°, indicated in figure 6a, with a measurement made every 0.5°. The receive antenna was then considered to be positioned at twice the peak abscissa value relative to the transmitter. This measurement, after the mixer response is subtracted, was used as the calibration for determining the amount of power and location of subsequent peak measurements. Figure 7 shows the calibration measurement for the data to be presented. The ordinate is a measure of the ratio of the analyzer's received IF to the analyzer's generated IF, and hence is in decibels. The noise level is considered to be -75 dB. The peak at 41.5° is a specular reflection indicating that the transmit and receive antennas are separated by 83°, i.e., 7° from perpendicular. Table 1 conveys the pertinent information for the two plots.

Figure 7. Calibration measurement of flat aluminum plate.

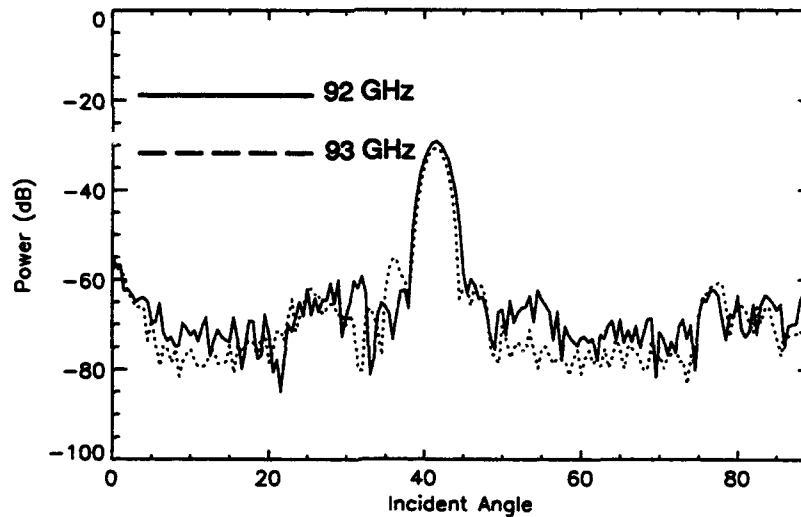


Table 1. Calibration plot parameters.

Frequency (GHz)	Peak power (dB)	θ_{3dB} (°)	Peak center (°)
92.5	-29.18	2.0	41.50
93.5	-30.66	2.0	41.50

Figure 8 is a 0 to 90° measurement of the grate with a resolution of 0.5°. Figures 9, 10, and 11 are measurements of the individual peaks with a resolution of 0.1°. Peak information is presented in table 2. The data show a shift of 0.3° in the θ_{3dB} beamwidth of the first peak (the half power point) and a 0.7° shift in the last peak for a 1-GHz change in frequency. The center peak does not appear to shift.

The order the energy has been directed into is known because we know the separation of the two antennas. Specifically, for each θ_i , which is taken to be the center of the θ_{3dB} beamwidth, the corresponding θ_o must be on the opposite side of the surface normal. Except for the center peak of figure 8, this is the $m = \pm 1$ order. Hence, the first and last peaks are images. The wider width and lower amplitude of the last peak are due to the changing aperture as the grate is rotated. The center peak is troublesome, because it does not seem to fit with the theory. Figures 12, 13, and 14 are repeats of the measurement of figure 8, except that polarization has been changed in steps of 15° (i.e., 15°, 30°, and 45° polarization measurements, respectively). Peak parameters are listed in table 3. These measurements show the polarization dependence of the directed energy. The center peak shows little variation with polarization, indicating that it is a flat plate specular reflection corresponding to $m = 0$.

Figure 8. 0 to 90° measurement of grate. Resolution is 0.5°. Peak information is listed in table 2.

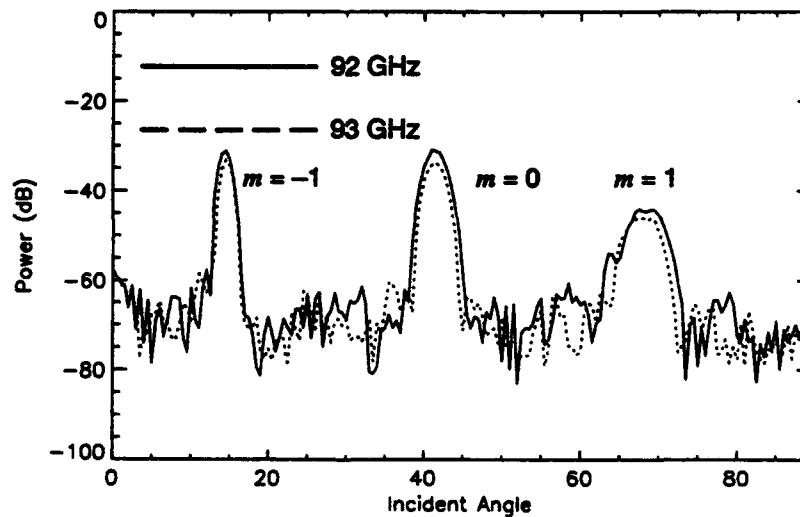


Figure 9. $m = -1$ of figure 8. Shift is detectable but not distinct.

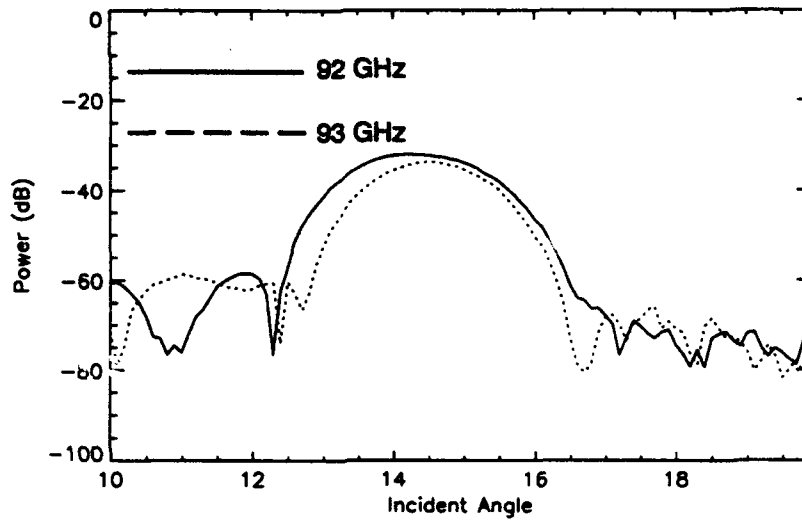


Figure 10. $m = 0$ of figure 8. There is no discernible shift.

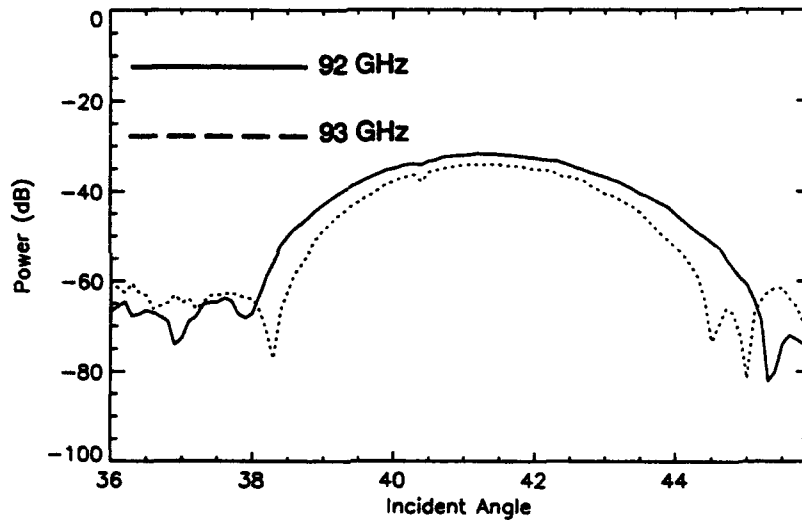


Figure 11. $m = 1$ of figure 8. Note that shift is in opposite direction and is more distinct than that of $m = -1$ peak.

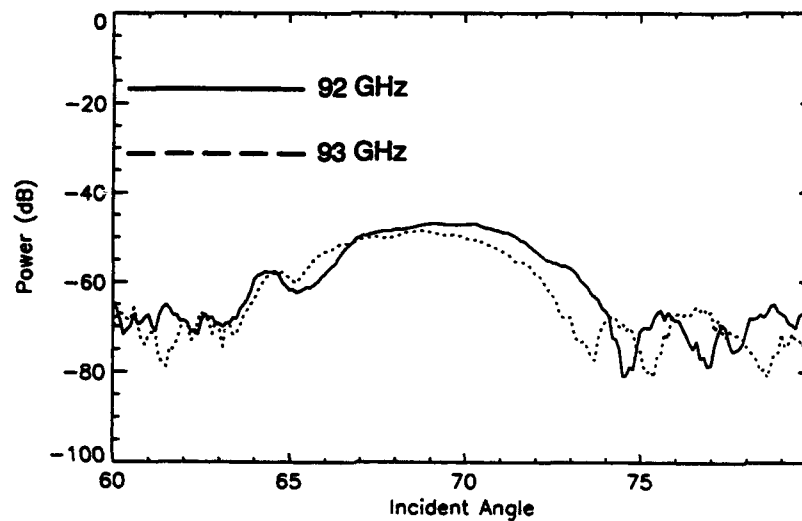


Table 2. Figure 8 peak parameters.

Frequency (GHz)	m^{th} peak	Power (dB)	$\theta_{3\text{dB}}$ ($^{\circ}$)	Peak center ($^{\circ}$)
92.5	-1	-31.96	1.5	14.20
92.5	0	-31.66	2.4	41.35
92.5	1	-46.97	4.3	69.25
93.5	-1	-33.72	1.2	14.50
93.5	0	-34.10	2.3	41.35
93.5	1	-48.48	3.9	68.55

Figure 12. 15° polarization measurement.

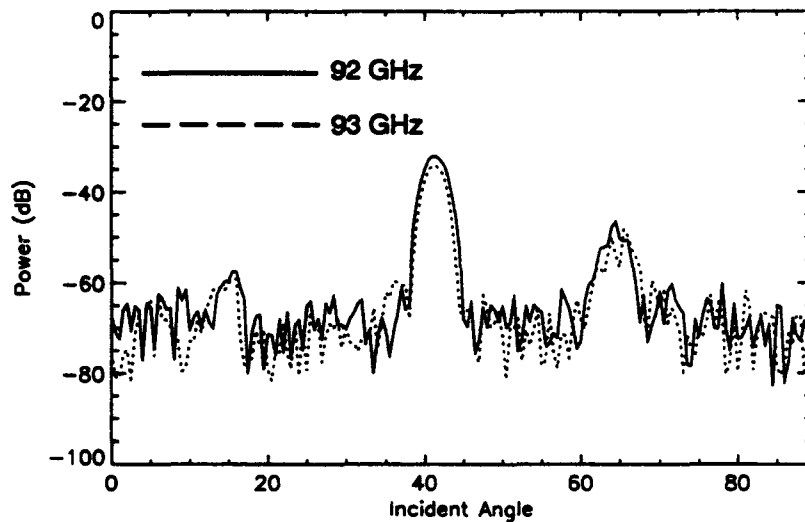


Figure 13. 30° polarization measurement.

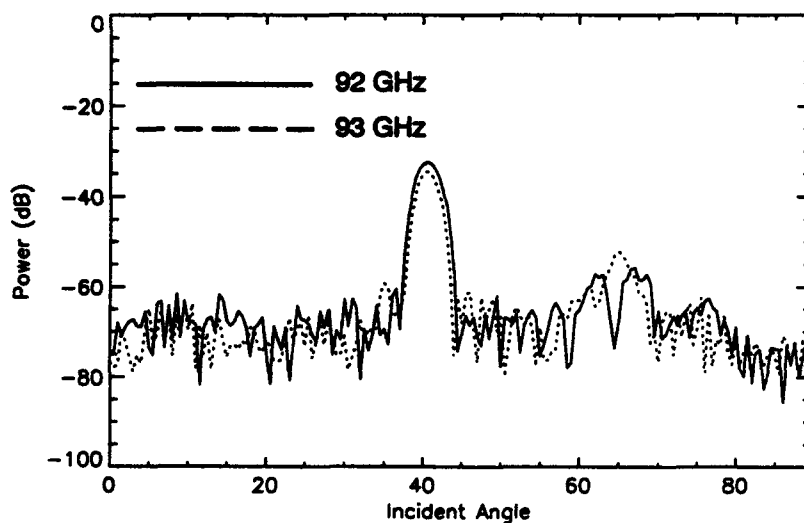


Figure 14. 45° polarization measurement.

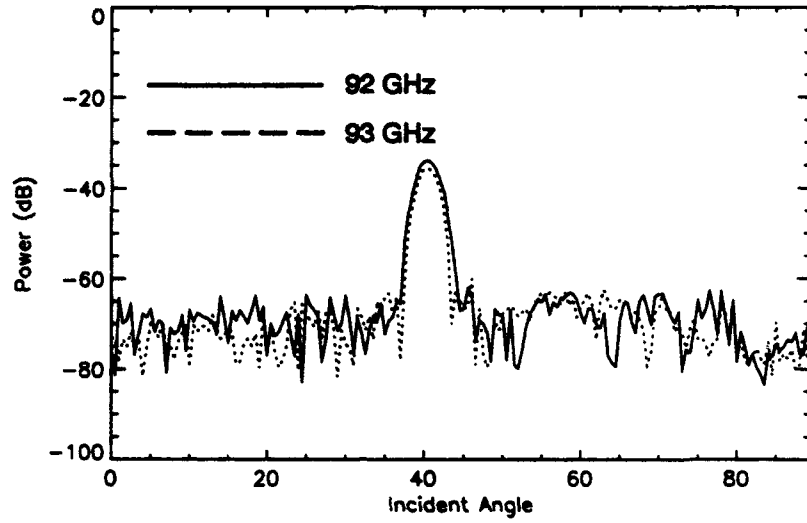


Table 3. Peak power polarization dependence for angles 15°, 30°, and 45°.

Frequency (GHz)	<i>m</i> th peak	Polarization angle (dB)		
		15°	30°	45°
92.5	-1	-56.36	NA	NA
92.5	0	-31.30	-32.07	-33.83
92.5	1	-49.82	-55.59	NA
93.5	-1	-59.96	NA	NA
93.5	0	-34.12	-34.33	-35.62
93.5	1	-51.31	-52.62	NA

6. Conclusions

The results of this experiment indicate that the optical theory of diffraction and blazed diffraction gratings may be scaled to MMW radiation, with some limitations. It has been shown that the shift of energy associated with blazed gratings is detectable. For the grating presented in this study, a 0.3° shift in the negative first-order beam was realized for a 1-GHz change in transmitted frequency. By choosing an appropriate geometry for the transmit-antenna/grating/receive-antenna system, along with the corresponding grating parameters (i.e., the blaze angle and the facet separation), one should be able to devise a beam sweep useful for guidance applications. Also, when the bandwidth of the transmitted frequency is increased, there is a concomitant increase in beam sweep. The presence of the $m = 0$ peak in the grating measurements is associated with the specular reflection from a flat plate. This indicates that the scalar theory of diffraction is inadequate when the facet separation is on the order of a wavelength ($l = 1.5 \lambda$ in this case). This anomaly need not be a hindrance for the application of this concept to guidance, in that the geometry of the system should be specified so that $\theta_i, \theta_o = 45^\circ$.

Follow-on work to this study should include a configuration in which the incident angle is held constant while the position of the receiver is varied. This would allow a more thorough examination of the spectrum. Also, measurements out of the plane defined by the grating and antenna bore should be considered; these would allow further investigation of the polarization dependence that was shown to exist for energy in orders other than $m = 0$.

Acknowledgments

I would like to thank Timothy Burcham of ARL, without whose help this project would not have been completed. Also, Suzanne Stratton and H. Bruce Wallace are thanked for many thoughtful discussions and their editorial assistance.

Distribution

Administrator
Defense Tech Information Ctr
Attn: DTIC-DDA (2 copies)
Cameron Station, Bldg 5
Alexandria, VA 22304-6145

Institute for Defense Analyses
Attn: J. Ralston
1801 N Beauregard St
Alexandria, VA 22311

Director
Benet Weapons Lab
U.S. Army Armament RDE Ctr
Attn: SMCAR-CCB-TL
Watervliet, NJ 12189-4050

Night Vision & Electro Optics Lab
Attn: C2NVEO-RD-NV-GSD, T. Witten
FT Belvoir, VA 22060

Commander
U.S. Armament RDE Ctr
Attn: SMCAR-TDC (2 copies)
Attn: SMCAR-FSP-A1, M. Rosenbluth
Attn: SMCAR-FSF-BD, L. Yung
Picatinny Arsenal, NJ 07806-5000

U.S. Army Field Artillery School
Attn: ATSF-CSI
FT Sill, OK 73503-5000

Commandant
U.S. Army Infantry School
Attn: ATSH-CD-CSO-OR
FT Benning, GA 31905-5660

Commander
U.S. Army Missile Command
Attn: AMSMI-RD-AS-MM, M. Christian
Redstone Arsenal, AL 35898-5253

Director
U.S. Army TRADOC Analysis Command
Attn: ATRC-WSR
White Sands Missile Range, NM 88002-5502

U.S. Army Aviation Research & Technology Activity
Attn: SAVRT-R
Moffett Field, CA 94035-1099

Commander
U.S. Army Materiel Command
Attn: AMCDRA-ST
5001 Eisenhower Avenue
Alexandria, VA 22333-0001

Director
U.S. Army Missile Command (USAMICOM)
Attn: AMSMI-RD-CS-R, Documents
Redstone Arsenal, AL 35898-5400

Commander
U.S. Army Tank-Automotive Command
Attn: ASQNC-TAC-DIT, Tech Information
Warren, MI 48397-5000

USACECOM
Attn: AMSEL-RD-EW-R, J. Borowick
FT Monmouth, NJ 07703

Naval Surface Warfare Ctr
Attn: Code F41, D. Marker
Attn: Code F41, J. Morrisett
Dahlgren, VA 22448-5000

Air Force Armament Lab
Attn: WL/MNOI
Eglin AFB, FL 32542-5000

Commander
Naval Weapons Center
Attn: Code 3954, S. Ghaleb
China Lake, CA 93555

Drexel University Physics Dept
Attn: T. W. Mercer
32nd & Chestnut Sts
Philadelphia, PA 19001

Distribution

Georgia Tech
Attn: M. T. Tuley
GTRI/MAL, CRB-564
Atlanta, GA 30332

Rensselaer Polytechnic Institute
Physics Dept
Attn: C. Ventrice
110 8th St
Troy, NY 12180

Stevens Institute of Technology
EECS Dept
Attn: S. H. Smith
Hoboken, NJ 07030

University of Nebraska
Electrical Eng Dept
Attn: R. Narayanan
Mail Stop 0511
Lincoln, NE 68588

Balanced Technology Init
Attn: P. Kicos
1901 N. Beauregard St
Alexandria, VA 22311

Coleman Research Corp
Attn: C. Barrett
3950 Lakehurst Dr
Orlando, FL 32819

MIT Lincoln Lab
Attn: S. Ayasli, Rm B-364
Attn: J. G. Fleischman, Rm B363
Attn: P. Reynolds, Rm A082
244 Wood St
Lexington, MA 02173

Rockwell International Corp
MMW Radar Technology
Tactical Syst Div
Attn: R. H. Wright, MS-DD46
3370 Miraloma Ave, PO Box 3170
Anaheim, CA 92803-3170

Rockwell International Corp
Attn: K. Hull, DC-04
3370 Miraloma Ave
Anaheim, CA 92803

Science & Tech Assoc
Attn: A. Glasser
4001 Fairfax Ave, Ste 700
Arlington, VA 22203

Technology Service Corp
Attn: B. Graziano
6515 Main St
Trumbull, CT 06611

U.S. Army Research Lab
Attn: AMSRL-OP-SD-T, Tech Library
(3 copies)
Attn: AMSRL-OP-SD-TM, Mail & Records
Mgmt
Attn: AMSRL-OP-SD-TP, Tech Pub
Attn: AMSRL-SS-I, Chief
Attn: AMSRL-SS-F, Chief
Attn: AMSRL-SS-SC, Chief
Attn: AMSRL-SS-SD, Chief
Attn: AMSRL-SS-SD, D. Bauerle
Attn: AMSRL-SS-SD, D. Wigner
Attn: AMSRL-SS-SD, S. Stratton
Attn: AMSRL-SS-SD, T. Burcham
Attn: AMSRL-SS-SD, T. Pizzillo (10 copies)
Attn: AMSRL-SS-SG, Chief
Attn: AMSRL-SS-SK, Chief
Attn: AMSRL-SS-SL, Chief
Attn: AMSRL-SS-SM, Chief
Attn: AMSRL-SS-S, Chief
Attn: AMSRL-SS-S, Director
Attn: AMSRL-SS-SA, Chief
Attn: AMSRL-SS-SD, E. Burke
Attn: AMSRL-SS-SH, Chief
Attn: AMSRL-SS-SH, J. Nemarich
Attn: AMSRL-SS-SJ, Chief
Attn: AMSRL-SS, J. Sattler